Deshraj Meena

Copy of final major report jitendra_deepesh_for plagiarism and AI check[1].docx - Google Docs

Phd Scholars

Document Details

Submission ID
trn:oid:::27535:140631651

Submission Date
May 27, 2026, 1:21 PM GMT+5:30

Download Date
May 27, 2026, 1:23 PM GMT+5:30

File Name
Copy of final major report jitendra_deepesh_for plagiarism and AI check[1].docx - Google Docs.pdf

File Size
1.9 MB

21 Pages

4,106 Words

22,993 Characters

5% Overall Similarity

The combined total of all matches, including overlapping sources, for each database.

Filtered from the Report

- Small Matches (less than 10 words)

28/05/2026

Match Groups

14 Not Cited or Quoted 5%
Matches with neither in-text citation nor quotation marks

1 Missing Quotations 0%
Matches that are still very similar to source material

0 Missing Citation 0%
Matches that have quotation marks, but no in-text citation

0 Cited and Quoted 0%
Matches with in-text citation present, but no quotation marks

Top Sources

3% Internet sources
4% Publications
2% Submitted works (Student Papers)

Integrity Flags

0 Integrity Flags for Review

Our system's algorithms look deeply at a document for any inconsistencies that would set it apart from a normal submission. If we notice something strange, we flag it for you to review.

A Flag is not necessarily an indicator of a problem. However, we'd recommend you focus your attention there for further review.

Match Groups

- **14** Not Cited or Quoted 5%
  Matches with neither in-text citation nor quotation marks
- **1** Missing Quotations 0%
  Matches that are still very similar to source material
- **0** Missing Citation 0%
  Matches that have quotation marks, but no in-text citation
- **0** Cited and Quoted 0%
  Matches with in-text citation present, but no quotation marks

Top Sources

3% Internet sources
4% Publications
2% Submitted works (Student Papers)

Top Sources

The sources with the highest number of matches within the submission. Overlapping sources will not be displayed.

1	Publication	
Wei Bai, Yi Zhou, Lingfang Xu, Haibo Xiao, Yang Tong, Chuangchuang He, Jinbiao ...		1%
2	Publication	
Uzair Naeem, Hao Li, Adil Alshoaibi, Dawei Wang et al. "Synthesis of SrTiO3 perov...		1%
3	Publication	
Shivani Sangwan, Vinod Singh, Deshraj Meena. "Optimizing dielectric and mecha...		<1%
4	Internet	
www2.mdpi.com		<1%
5	Internet	
www.metall-mater-eng.com		<1%
6	Student papers	
Chulalongkorn University on 2012-05-14		<1%
7	Publication	
Donghee Lee, Hyeongwoo Kim, Chaewon Kim, Bum Sung Kim, Woo-Byoung Kim. "...		<1%
8	Internet	
journal.bcrec.id		<1%
9	Internet	
www.mdpi.com		<1%
10	Internet	
f.oaes.cc		<1%

CHAPTER 1

INTRODUCTION

Nowadays, researchers are paying increased attention to advanced energy storage technologies due to the rapid dwindling of conventional fossil fuels and their associated environmental impacts [1]. Furthermore, the escalating demand for versatile, highly miniaturized components in microelectronics and modern pulsed-power devices like medical defibrillators , radar has sparked immense interest in eco-friendly, lead-free ceramics exhibiting colossal permittivity (CP)[2]. While traditional ceramic systems such as $BaTiO_3$, $Na_{0.5}Bi_{0.5}TiO_3$, and $CaCu_3Ti_4O_{12}$ (CCTO) often display inspiring CP values, they frequently struggle with severe property variations across different frequencies and operating temperatures [3]. These inherent fluctuations with high dielectric loss, severely limit their real-world device potential. That's why the advancement of lead-free ceramics that can sustain high permittivity (>10^4) with minimal dielectric loss (tan $\delta < 0.1$). And high temperature reliability holds critical value for next-generation energy storage applications [4].

Strontium titanate ($SrTiO_3$) is a prominent candidate that has been extensively explored due to its intrinsically low dielectric loss , amplified breakdown strength , and excellent high-temperature stability. A pure $SrTiO_3$ retain a relatively low intrinsic dielectric permittivity which used to be increased to meet advanced application requirements. Different types of theoretical models have been proposed to explain the origins of induced colossal permittivity in modified titanates. Mainly including the internal barrier layer capacitance (IBLC) effect, electron-pinned defect dipoles (EPDD), and surface barrier layer capacitance (SBLC) [5]. The co-existence of these mechanisms shows a significant challenge in selecting the optimal pathway for material modification. Therefore, developing an effective approach to consistently enhance the dielectric properties of $SrTiO_3$ Ceramics provide ample practical benefits [6].

Defect engineering that used to provide a highly controlled approach to introducing specific point defects ranks among the most efficient methods for modifying dielectric behavior [7]. A leading technique involves slipping site-occupying point defects into the crystal lattice via acceptor and donor ion doping [8, 9]. In this study, tantalum (Ta^{5+}) is employed as an aliovalent donor dopant to modify the $SrTiO_3$ lattice site . A strategy specifically designed to secure the high-frequency stability and temperature reliability. By Utilizing this defect engineering along with an optimized solid-state reaction process using that Ta-doped $SrTiO_3$ (STTO) ($SrTi_{0.997}Ta_{0.003}O_3$) ceramics were prepared particular targeting the stoichiometric formulation of $SrTi_{0.997}Ta_{0.003}O_3$.

The Ta doped $SrTiO_3$ is widely appreciated for its excellent room-temperature dielectric properties that attain high permittivity along with a strictly maintained low tanδ. Due to its vigorous permittivity and the environmental advantages of being a lead-free material the STTO is highly preferred for the integration of multilayer ceramic capacitors (MLCCs) [10]. To maintain production , scalability and reliability throughout the growing demand for MLCCs with higher capacitance and smaller footprints. The primary challenge lies in advance optimizing its dielectric performance . Previous studies indicate that the overall dielectric constant and breakdown strength can be enhanced by reducing the grain size to a critical threshold. Thereby limiting long-range leakage currents and domain wall movement [11]. Thus, it is mandatory to evolve methods that effectively control grain growth during sintering without compromising the macroscopic dielectric properties [12].

While modern efforts have employed various sintering additives to tackle these issues. The core-shell architectures have emerged as a far superior solution to evenly distribute these additives at the nanoscale. This overcomes the inhomogeneity problems inherent to traditional ball-milling methods. Coating a thin shell around the highly polarizable STTO core ensures a homogenous spread of secondary phases which boosts densification and tightly controls grain

growth during the sintering process. If conventional low-permittivity materials (such as SiO_2, TiO_2 or MgO) are used as the shell then they can drastically suppress the overall macroscopic performance of the composite in spite of their microstructural gains [13, 14 ,15]. To enhance the dielectric properties while strictly constraining grain growth, this study employs a super-thin TiO_2 shell applied via a peroxo titanium complex (PTC) precursor.

This study focuses on engineering a core–shell Ta-doped $SrTiO_3$@PTC structure tailored explicitly for high-frequency capacitor applications. In this core-shell Structural design, the Ta-doped $SrTiO_3$ acts as a core and PTC-derived boundary layer functions as an internal capacitive barrier. By physically isolating the highly polarizable STTO grains, this insulating shell effectively disrupts macroscopic leakage current pathways and mitigates detrimental interfacial polarization. This research investigates the microstructural evolution and dielectric mechanics of the STTO@PTC system and aims to demonstrate that precise core-shell encapsulation can suppress high-frequency dielectric loss. Also presenting a robust dielectric constant thereby delivering a highly optimized lead-free dielectric for next-generation pulsed-power and energy storage devices.

CHAPTER 2

LITERATURE REVIEW

2.1 Overview: Strontium titanate ($SrTiO_3$)

Strontium titanate ($SrTiO_3$) is a perovskite-structured material. It has gained attention due to its advantageous stable dielectric properties, electronic tunability, and chemical stability [16, 17]. $SrTiO_3$ plays a vital role in fuel cells by enhancing ionic conduction and improving the stability of electrodes [18]. It also serves as a promising material in different types of supercapacitors, utilizing its large surface area and charge storage capabilities to boost the energy density and improve capacitance [19]. The structure of strontium titanate shows a perovskite ABO_3 structure, with TiO_6 octahedra surrounded by strontium atoms. It used to exhibit a cubic structure above 105 K and transitioned to a different structure below this temperature. Doping in $SrTiO_3$ with cations of higher oxidation states enhances conductivity by generating electrons and vacancies, which helps to maintain charge balance in the perovskite structure and this results used in improving both electronic and ionic properties [20, 21, 22]. These features of $SrTiO_3$ make it suitable core material for synthesizing dielectric composites such as core-shell structure.

2.2 Ta Doping in $SrTiO_3$

Pure $SrTiO_3$ is a quantum Paraelectric material with a high dielectric constant which increases at low temperatures. Its dielectric permittivity at room temperature remains stable , and dielectric loss can increase under frequency or temperature fluctuations [23, 24]. To overcome these limitations, doping strategies have been widely investigated. Among all the donor dopants, tantalum (Ta^{5+}) stands out due to its ability to substitute Ti^{4+} sites within the lattice . Because the ionic radius of Ta^{5+} is slightly larger than that of Ti^{4+} that causes measurable lattice expansion and shifting XRD peaks to lower angles, confirming successful doping [19]. This substitution of tantalum introduces positively charged donor states and triggers the formation of

defect dipole clusters, such as $Ti^{'} - V_{0}^{..} - Ti^{'}$ and $Ta. - V_{0}^{..} - 3Ti^{'}$, which enhance local polarization and significantly improve dielectric performance [25, 26]. STTO (Ta doped $SrTiO_3$) ceramics have been reported to exhibit colossal permittivity ($\varepsilon_r \approx$ 11,423 at 1 kHz) and remarkably low dielectric loss , which are refer to electron-pinned defect dipole (EPDD) effect mechanisms and controlled oxygen-vacancy complexes [25, 26].

In spite of these remarkable properties, STTO still suffers from many issues such as leakage currents, microstructural inhomogeneity, and grain-boundary conduction losses at higher frequencies. These limitations necessitate additional structural control, where core–shell engineering becomes a highly effective approach.

2.3 Core–Shell structure for Dielectric Optimization

Core–shell structures have gained prominence for tailoring electrical responses in dielectric materials by containing a high-permittivity core with an insulating or semi-insulating shell. It is used to simultaneously accomplish :

- ➔ Improved interfacial polarization
- ➔ Enhance thermal stability
- ➔ Depletion of dielectric loss
- ➔ Management of microstructural heterogeneity

For $SrTiO_3$-based dielectrics , the core–shell abstract idea allows the high intrinsic permittivity of the core to be retained while engineering an insulating shell that limits conduction losses [27]. This structure also raises a Maxwell–Wagner interfacial polarization effect, which can further upgrade effective permittivity.

Peroxo Titanium Complex (PTC) Material shows strong resistivity modulation due to grain-boundary barrier layers when it used as a shell substance around high-k $SrTiO_3$ particles it serve multiple beneficial functions [15] :

-→They make a resistive boundary layer that blocks charge jumping and leakage currents, effectively reducing dielectric loss.

-→ Thermal stability is enhanced as PTC materials naturally exhibit temperature-driven resistance increases , stabilizing dielectric behaviour.

2.4 Research Gap and Motivation for Ta doped $SrTiO_3$@PTC Core–Shell Design

→ Grain-boundary conduction can still contributed to the dielectric loss.

→ Leakage pathways are affected by the colossal permittivity of the materials.

→ Frequency-dependent response requires enhanced control of microstructural heterogeneity.

core–shell engineering Ta doped $SrTiO_3$@PTC offers better solutions to these challenges but remains underexplored. The combination of Ta-doped $SrTiO_3$ as the core with a PTC shell acting as a resistive barrier represents a powerful approach for achieving high permittivity as well as low dielectric loss, which is indispensable for next-generation energy storage devices and high-frequency capacitor applications.

CHAPTER 3

EXPERIMENTAL

3.1 Material and Reagents

Raw materials including Strontium Hydroxide Octahydrate ($Sr(OH)_2.8H_2O - 99.96$ % purity), Titanium Dioxide ($TiO_2 - 99.94\%$ purity), Tantalum Penta-oxide($Ta_2O_5 - 99.99\%$) purchased from (Sigma Aldrich). Hydrogen Peroxide ($H_2O_2 - 99.4\%$) as Oxidizing agent, Titanium Hydride ($TiH_2 - 99.9\%$), Ammonium Hydroxide($NH_4OH - 99.9\%$)as base catalyst, 5% PVA as binder and Deionized water (DI) water.

Solid State Synthesis:

Solid state synthesis commonly referred to as the ceramic method chemical process in which a new solid compound having an already known structure is synthesized using solid precursors. The products derived from this process are widely used in the energy and electrical area. These products cover polycrystals, single crystals, glasses and thin-film materials.

The overall concept is that the fine-grain metallic mixture is homogenised pressed to make pellets which then is heated for a particular temperature for a particular time. Some metal compounds for example, metallic oxides in combination with salts require harsh environments like high pressure and temperature for processing either as a melted flux or a rapid condensing vapor phase.

Evaluation of rate of reaction in solid state process is very important because purification methods available to recover these solid products are extremely poor, so the reactions must be carried out until the completion.The rate of reaction in solid state synthesis is dependent on lots of factors such as structure factors, arrangement and rate of diffusion and thermodynamics concerning reactions.

3.2 Synthesis Methods

3.2.1 synthesis of $SrTi_{1-x}Ta_xO_3$ ceramics (x=0.3wt%) nanoparticles

$SrTi_{1-x}Ta_xO_3$ (x=0.3wt%) has been prepared using the solid- state reaction method, abbreviated as STTO. Based on the pretended stoichiometric ratio of the target compound, the raw materials such as $Sr(OH)_2.8H_2O, TiO_2$ and Ta_2O_5 were accurately weighted. The mixture was grinded in the mortar and pestle with the help of DI water for 12 hours to achieve uniform mixing. After completing the initial hand grinding, the resulting powder was dried and calcined at 1150˚C for 2 hours. The calcined powder underwent another 12 hour hand grinding and followed by drying. Thus, we obtained $SrTi_{1-x}Ta_xO_3$(x=0.3wt%) nanoparticles, a schematic diagram have been shown in Fig.1.

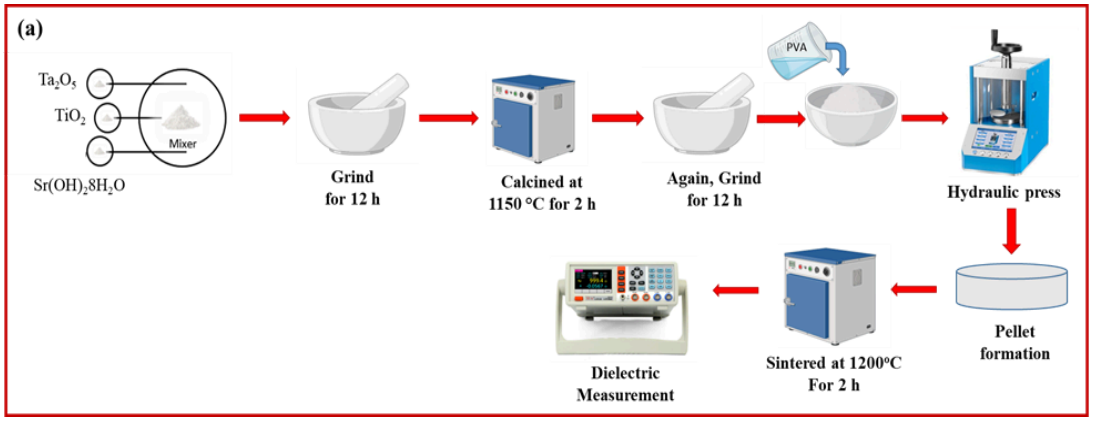

Fig. 1 Schematic representation for the synthesis of $SrTi_{1-x}Ta_xO_3$ (x=0.3wt%) (STTO)

3.2.2 Synthesis of PTC (peroxo titanium complex) Shell

To prepare the PTC solution for the shell layer, as shown in Fig. 2, 10 ml of H_2O_2 (oxidizer) kept on stirring for 40 minutes in a jacketed beaker at 50˚C temperature. During this process 25 mg of TiH_2 and a little drop of NH_4OH (base catalyst) was added to the solution . The resulted solution was again stirred in a jacketed beaker,

keeping the temperature below 50°C for 1h. Once the TiH_2 dissolved fully, a yellowish transparent solution was obtained, this was the PTC solution.

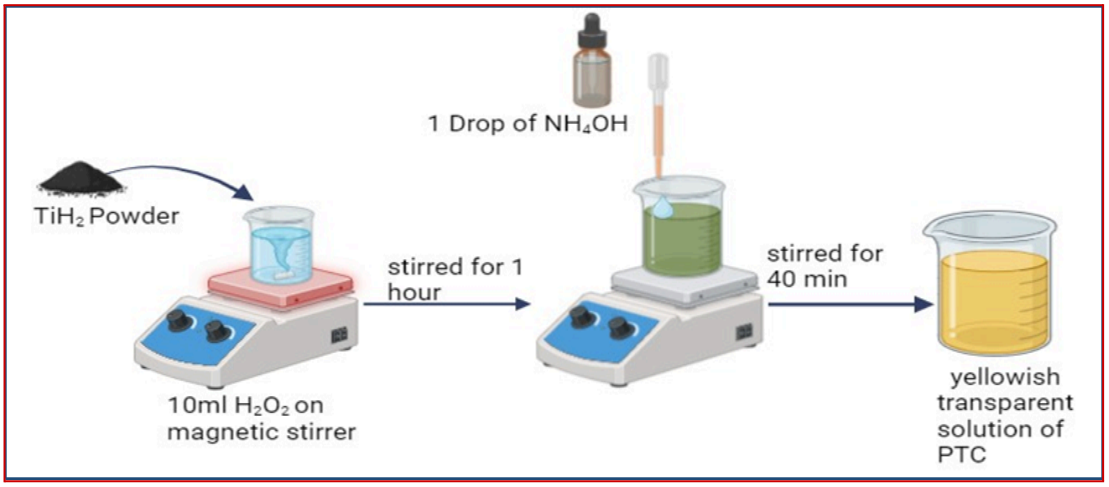

Fig. 2 Schematic representation for the synthesis of PTC (peroxo titanium complex)

3.2.3 Synthesis of Core-shell structured ($SrTi_{1-x}Ta_xO_3$ @ PTC) nanoparticles

For the coating of PTC shell on the surface of $SrTi_{1-x}Ta_xO_3$ (STTO), STTO powder was added to the deionized water (DI) and mixed by the bath ultrasonicator. Then the PTC solution was dropwise added to $SrTi_{1-x}Ta_xO_3$(STTO) suspension and stirred at 350 rpm at 70˚C for 12 hours. To investigate the microstructure and dielectric properties, PTC amount has been varied (3 and 5wt%) which will help to compare microstructure and dielectric trends of the nanoparticles. After completing the reaction, the dissolved STTO@PTC suspension was centrifuged and the precipitate has been collected to at 80˚C for 12 hours. After the natural cooling, we obtained core-shell structured (STTO@ PTC) nanoparticles.

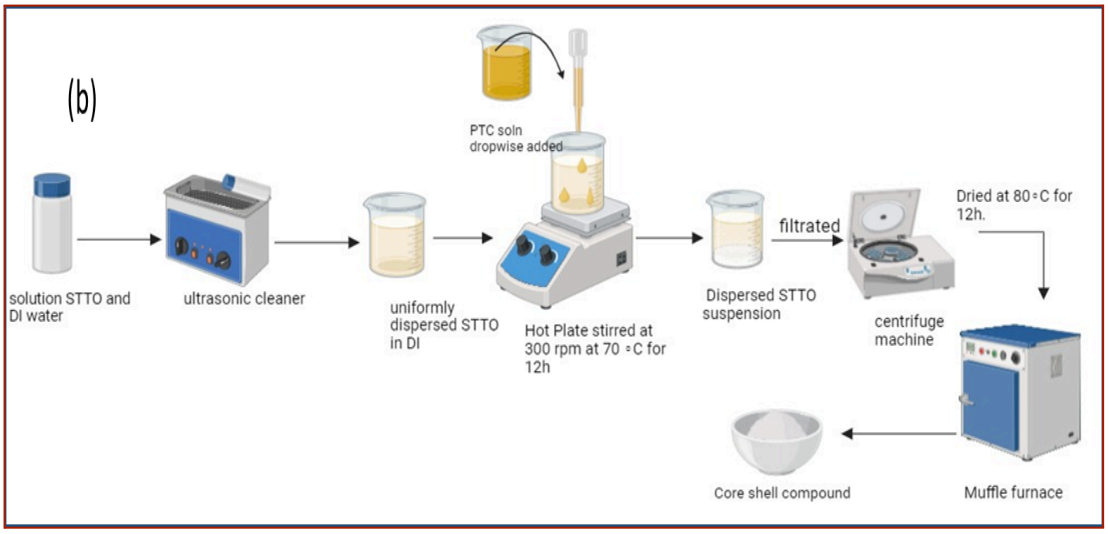

Fig.3 Schematic representation for the synthesis of core-shell structured STTO@PTC nanoparticles

3.3 Sintering

The fabricated PTC - coated STTO core -shell particles were compacted into pellets using uniaxial pressing via hydraulic press. The pellets of diameter 6 mm and a thickness of 1mm have been prepared under a pressure of 20 MPa. To improve the mechanical strength of a pellet, the organic PVA binder was used. The resulting pellets were then isothermally sintered at temperatures 1150˚C and 1200˚C for 2 hours, with a heating rate of 5˚C per minute.

CHAPTER 4

CHARACTERIZATIONS

4.1 Characterization Techniques

To confirm the crystal structure of synthesized samples, Bruker D8 Discover X – ray diffractometer with X – ray source of Cu K (1.54 Å) has been used. Perkin Elmer used to carry out Fourier Transform Infrared Spectroscopy (FTIR) which successfully identified the functional group and chemical bonding within Ta Doped $SrTiO_3$. Technai G2 T30, U-Twin Transmission Electron Microscope (TEM) was used to confirm the coating of PTC layer on STTO. Further, dielectric properties have been studied within a wide frequency (100Hz -2MHz) range at room temperature using a Hioki LCR meter (Model IM3536) and a PID temperature controller (Model 234).

4.2 Result and discussion

4.2.1 X- Ray Diffraction (XRD):

A non-destructive technique that analyses the atomic and molecular structure of a crystal and the crystallite size, phase and internal stress within micro crystalline regions is called X-ray crystallography.

Fig. 5 represents the XRD pattern of the synthesized Ta-doped $SrTiO_3$ and the core-shell structure STTO@PTC. The observed diffraction peaks of STTO (Fig. 5(a)) have been observed 22.8°, 32.22°, 40.0°, 46.30°, 52.5°, 57.63°, 68.6°, 72.5° and 78.° that correspond to (100), (110), (111), (200), (210), (211), (220), (221), and (310) planes and has been matched with JCPDS file No. 35-0734. It is found that all samples show a pure cubic perovskite phase with space group Pm-3m [28, 29]. The observed result shows that during the synthesis of STTO, the Ta ions have been successfully consolidated into the crystal lattice of $SrTiO_3$, producing a slight shift in (110) diffraction peak [29]. Fig. 5(b) and 5(c) show the XRD patterns of the calcined STTO@PTC core-shell structure with 3wt% and 5wt% of PTC, respectively.

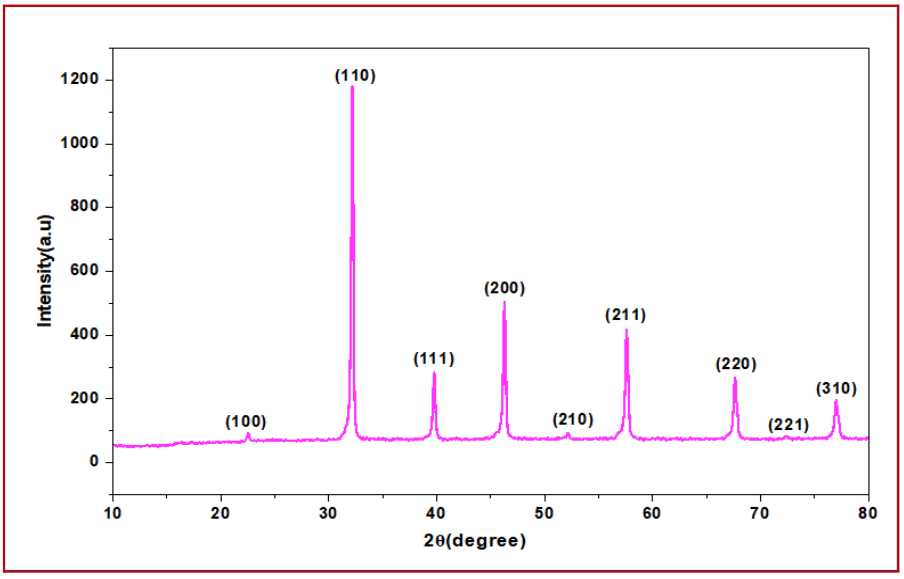

Fig. 4 XRD of Ta Doped $SrTiO_3$ with 3wt% Ta Doping.

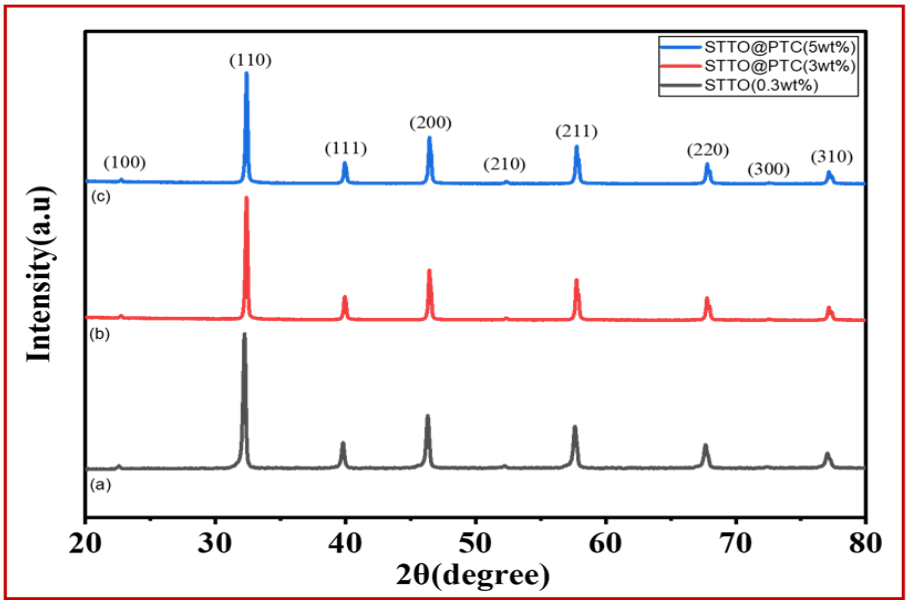

Fig. 5 XRD patterns of the synthesized (a) STTO nanoparticles, (b) calcine core-shell STTO@PTC powder (3wt%), (c) calcined core-shell STTO@PTC powder (5wt%)

The diffraction patterns closely match with the crystalline $SrTiO_3$ and no secondary phases have been detected [30]. Concurrently, the absence of macroscopic crystalline TiO_2 reflections suggests that the peroxo titanium complex (PTC) precursor may have formed an amorphous or finely dispersed nanoscale boundary layer at the STTO particles interfaces as there are no specific crystalline peaks for TiO_2 in XRD patterns of STTO@PTC [31].

There is a small shift in (110) diffraction peak. This peak shift leads to the larger ionic radius of Ta^{5+} compared to Ti^{4+}. Due to the substitution of Ta^{5+} in the place of Ti^{4+} interplaner increases and this results in an increase in the volume of the unit cell.

To calculate the crystallite size of synthesized material Scherrer's formula was used, the formula given as

$$D = \frac{K\lambda}{\beta Cos\theta} \quad (1)$$

Where,

D = Crystallite Size

K= Shape factor = 0.9

$\lambda = Wavelength\ of\ CuK_\alpha$ (1.54 A°)

$\beta = FWHM$

θ = Bragg's angle

The average crystallite size was found 63 nm. This size of crystallites represent that very fine nanoparticles were created. Further for calculating microstrain present in the nanoparticles 'Uniform Deformation Method' was used and with the help of the Willum -Hall plot which is given in figure.5 microstrain successfully calculated. The following Scherrer equation with strain given as

$$\beta_{total} = \frac{K\lambda}{D\cos\theta} + 4\varepsilon tan\theta \quad (2)$$

Or

$$\beta cos\theta = 4\varepsilon sin\theta + \frac{K\lambda}{D} \quad (3)$$

where, β is the Full width at half maximum , θ is the Braggs angle and ε is the slope of the W-H plot where it represents the microstrain present in the nanoparticles. $\frac{K\lambda}{D}$ is the intercept in the W-H plot which is used to calculate crystallite size.

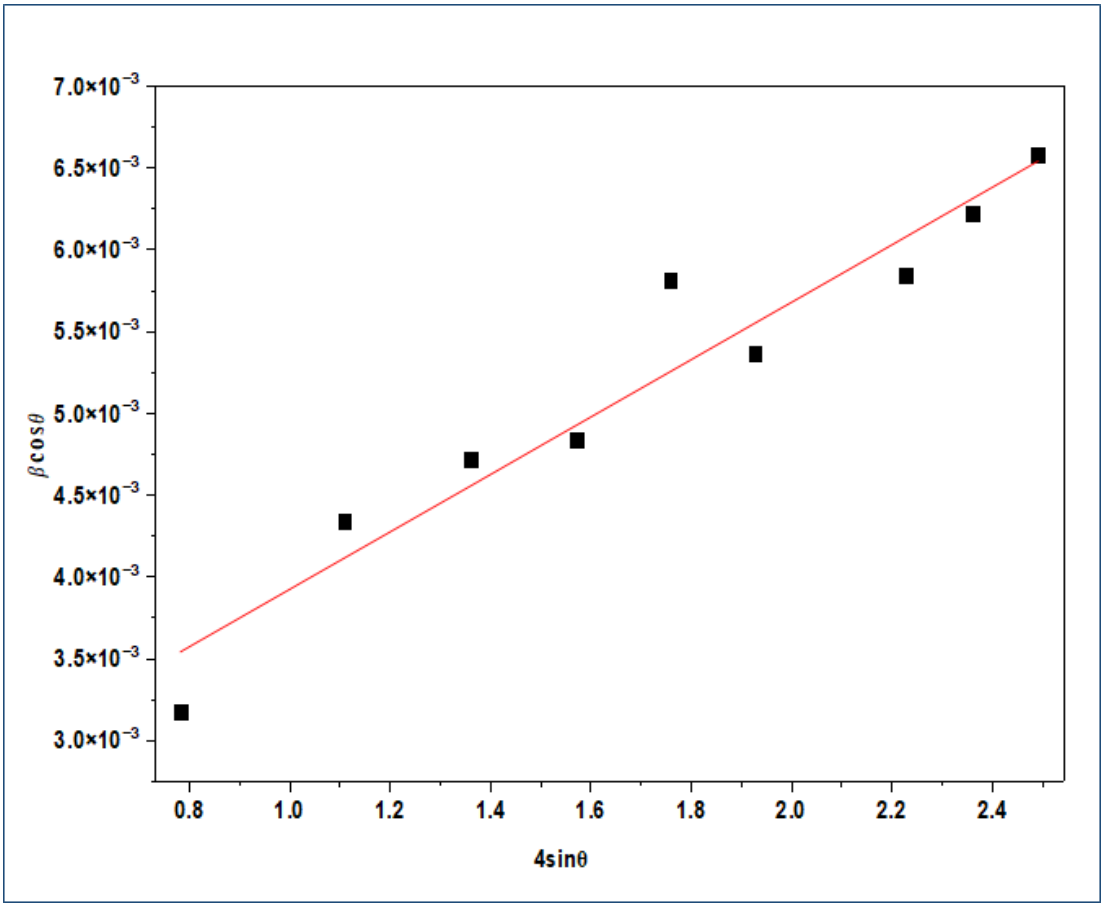

Fig. 6 W-H Plot using X- Ray Diffraction (XRD) Data

4.2.2 Fourier Transform Infrared Spectroscopy (FTIR):

Fourier Transform Infrared (FTIR) spectroscopy was utilized to evaluate the chemical bonding and surface characteristics of the Ta-doped $SrTiO_3$ (STTO) powder. Fig. 7 represents the FTIR spectra for the synthesized samples. The low-frequency region of the spectrum exhibits robust absorption bands at 525 cm^{-1}, 480 cm^{-1}, and 855 cm^{-1} which correspond to the characteristic stretching vibration of $Sr-Ti-O$, bending vibrations of $Ti-O$, and stretching of $Ti-O_6$ octahedra, respectively [32]. Because the doping concentration was so incredibly tiny (0.3wt%), and because Ta and Ti have relatively similar atomic properties, the vibration of the $Ta-O$ bond is practically identical to the $Ti-O$ bond [33]. Further, the infrared peak at 1485 cm^{-1} indicates hydroxyl (-OH) group from the adsorbed water [32]. Because these polar surface species can act as charge trapping centers and facilitate surface ionic conduction that inherently increases dielectric loss under high-frequency alternating electric fields [34].

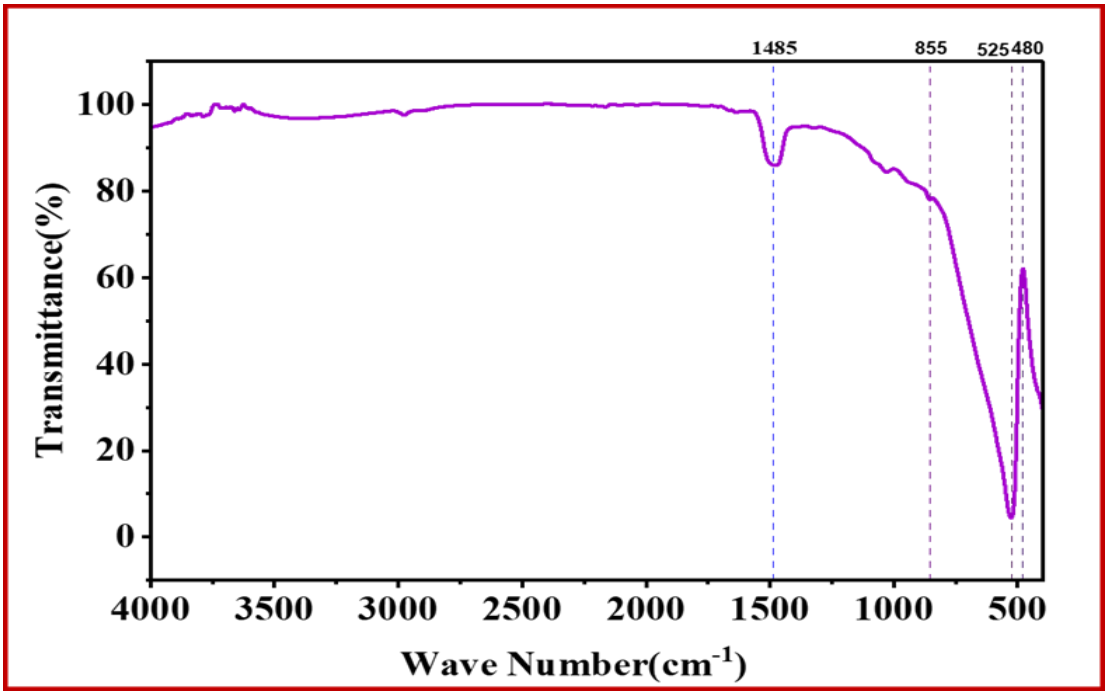

Fig. 7 Fourier Transform Infrared (FTIR) Spectroscopy of the base $SrTi_{1-x}Ta_xO_3$ (x=0.3%) STTO powder

4

4.2.3 TEM analysis:

Transmission Electron Microscopy (TEM) was employed to visually confirm the morphological evolution and structural encapsulation of the STTO@PTC composites. Fig. 8 shows the illustrative demonstration of the prepared core–shell structured STTO@PTC nanoparticles (Fig. 8(a)) with their morphological features as revealed by TEM images. The highly - magnified TEM images as shown in Fig.8 (b-d), certainly reveals a distinct core–shell structure ,characterized by a dark , electron-concentrate (STTO) core enveloped by a lighter colour i.e., amorphous-like Peroxo Titanium Complex (PTC) derived as TiO_2 shell. The calculated shell thickness is uniformly maintained at approximately 32 nm , clearly defined by the mass-thickness contrast between the crystalline- core and the applied boundary

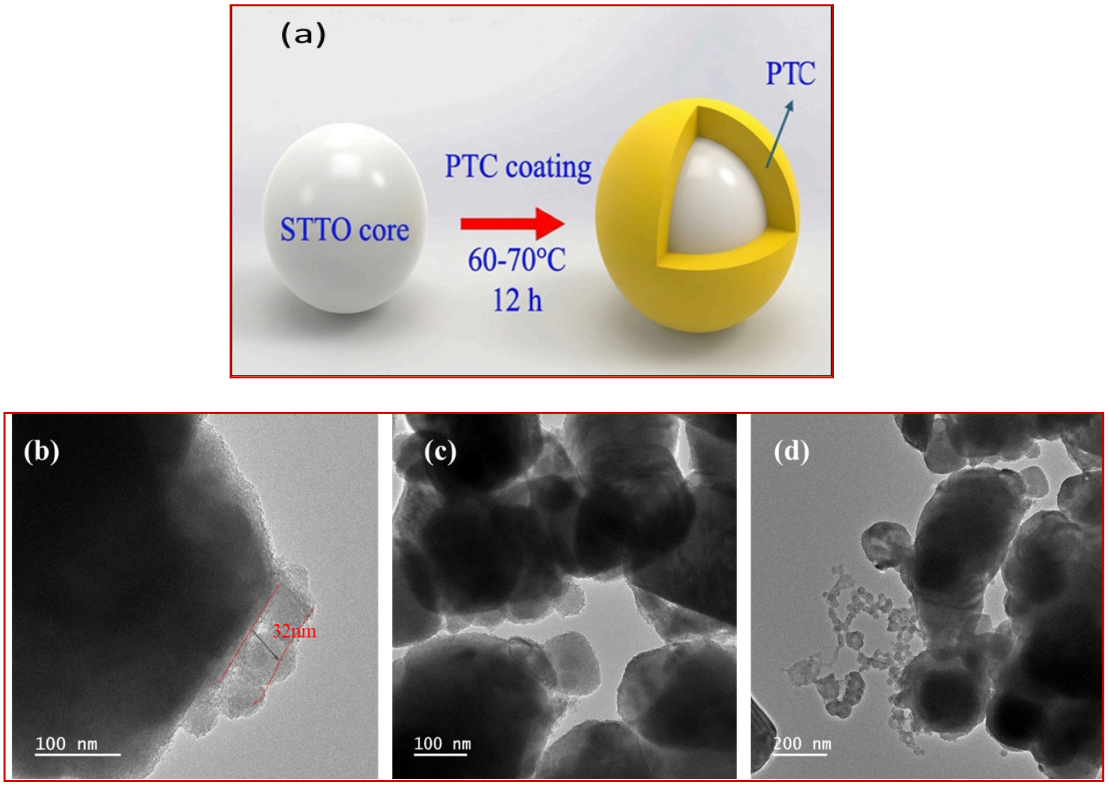

Fig. 8 (a) The illustrative representation of core-shell structure , (b-d) TEM images of STTO@PTC Core-shell structure at different scale of magnifications

coating [35]. These TEM images illustrate that this encapsulating layer successfully covers the individual base (STTO) particles , avoiding direct physical contact

between the highly polarizable STTO cores [36]. From a dielectric engineering point of view , this ~32 nm wide continuous interfacial layer is of key importance for high-frequency capacitor applications.

It behaves as an analytical , structural and electrical barrier that hinder long-range charge carrier transport and interfacial polarization. By physical isolation of STTO grains, the PTC shell successfully disrupts continuous leakage currents pathways , thereby suppressing dielectric loss (tan(δ)) and intensely enhancing the overall breakdown strength of the prepared composite [37].

4.2.4 Dielectric studies :

Fig. 9 shows, The frequency dependence of the dielectric constant (K or ε′) and dielectric loss (tanδ) for the $SrTi_{1-x}Ta_xO_3$ @ PTC nanoparticles sintered at 1200˚C at room temperature across a high-frequency range (100Hz–2000 kHz). As depicted in the fig. 8a, the base STTO core exhibits the highest dielectric constant (K≈160) that remains remarkably stable across the measured frequency spectrum. Upon encapsulation with the PTC-derived TiO_2 shell the effective permittivity of the composites drastically decreases. The STTO@PTC (3wt%) sample exhibits dielectric constant K≈50 while the 5wt% sample stabilizes near K≈70 at higher frequencies.

The highly polarizable STTO grain and the insulating TiO_2 boundary layer acts as two capacitors in series. This behavior is mathematically described by the classic series mixing model for Internal Barrier Layer Capacitors (IBLC):

$$\frac{1}{C_{total}} = \frac{1}{C_{core}} + \frac{1}{C_{shell}} \quad (4)$$

In terms of effective permittivity (ε_{eff}) and volume fractions (V):

$$\varepsilon_{eff} = \frac{\varepsilon_{core}\varepsilon_{shell}}{V_{core}\varepsilon_{shell} + V_{shell}\varepsilon_{core}} \quad (5)$$

Because the intrinsic permittivity of the amorphous/nanocrystalline TiO_2 shell is lower than that of the Ta-doped $SrTiO_3$ perovskite core, the low-permittivity shell dominates the denominator. This shell acts as an electrostatic bottleneck that inherently reduces the macroscopic dielectric constant of the bulk material [38].

While the dielectric constant is reduced, the true advantage of the core–shell architecture is revealed in the dielectric loss spectrum (fig. 9b) . The dielectric loss or dissipation factor represents the ratio of dissipated electrical energy to stored energy:

$$tan\delta = \frac{\varepsilon''}{\varepsilon'} \quad (6)$$

where ε'' is the imaginary part of permittivity and ε' is the real part of permittivity. Reducing this ratio is the primary objective for high frequency capacitor applications.

The STTO@PTC (3wt %) sample represents an exceptionally low and stable dielectric loss (TiO_2 < 0.02) across the entire 100Hz–2000 kHz range. This confirms that the shell layer generated at 3wt% successfully suppresses long-range leakage currents between STTO grains without introducing excessive defect states . By increasing the PTC shell concentration to 5 wt% induces a degradation in performance that characterized by a massive low-frequency loss spikes (TiO_2 > 0.20) and a sustained at high-frequency plateau (TiO_2≈0.05). This phenomenon is managed by Maxwell-Wagner-Sillars (MWS) interfacial polarization [34]. The variation in thickness of TiO_2 coating leads to an excessive accumulation of space charges at the STTO/TiO_2 interface. Under an alternating high-frequency electric field . The relaxation time (τ) of these trapped charges causes them to oscillate out of phase with the field and dissipating electrical energy as heated according to the Debye relaxation model:

$$\varepsilon''_{MWS} \propto \frac{\omega\tau}{1+\omega^2\tau^2} \quad (7)$$

where ω is the angular frequency.

At 5 wt%, the complete volume of oscillating interfacial charges massively inflates ε'', destroying the low-loss profile required for high-frequency efficiency [39]. Thus,

the frequency-dependent dielectric spectra indicate that the 3 wt% PTC coating provides

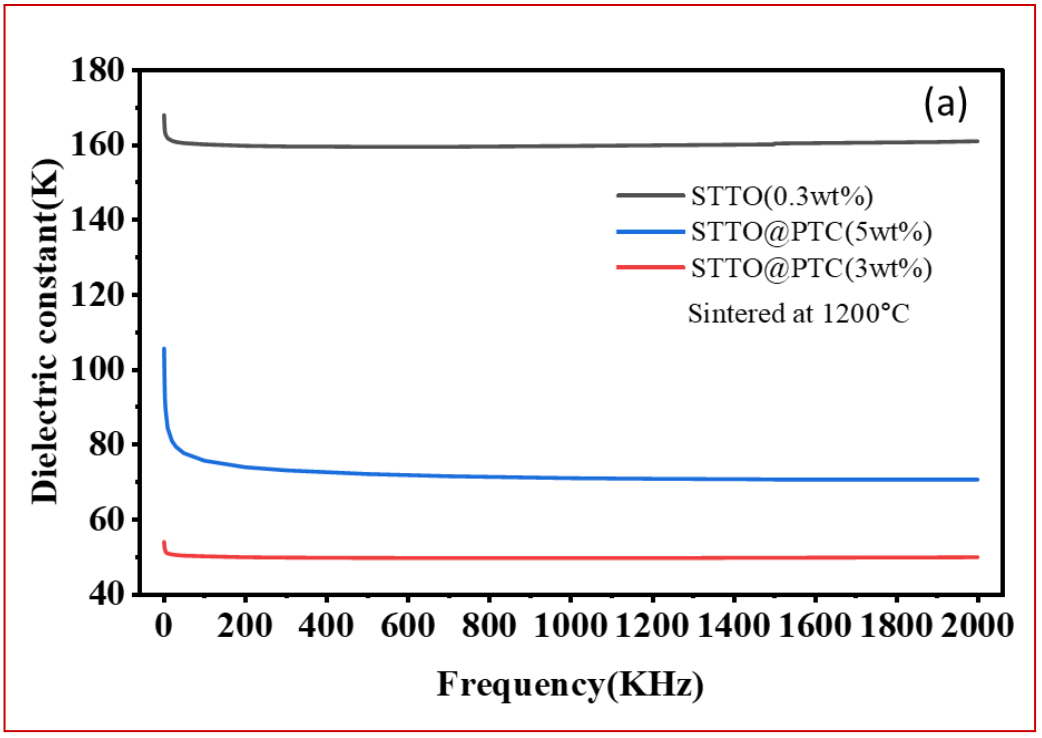

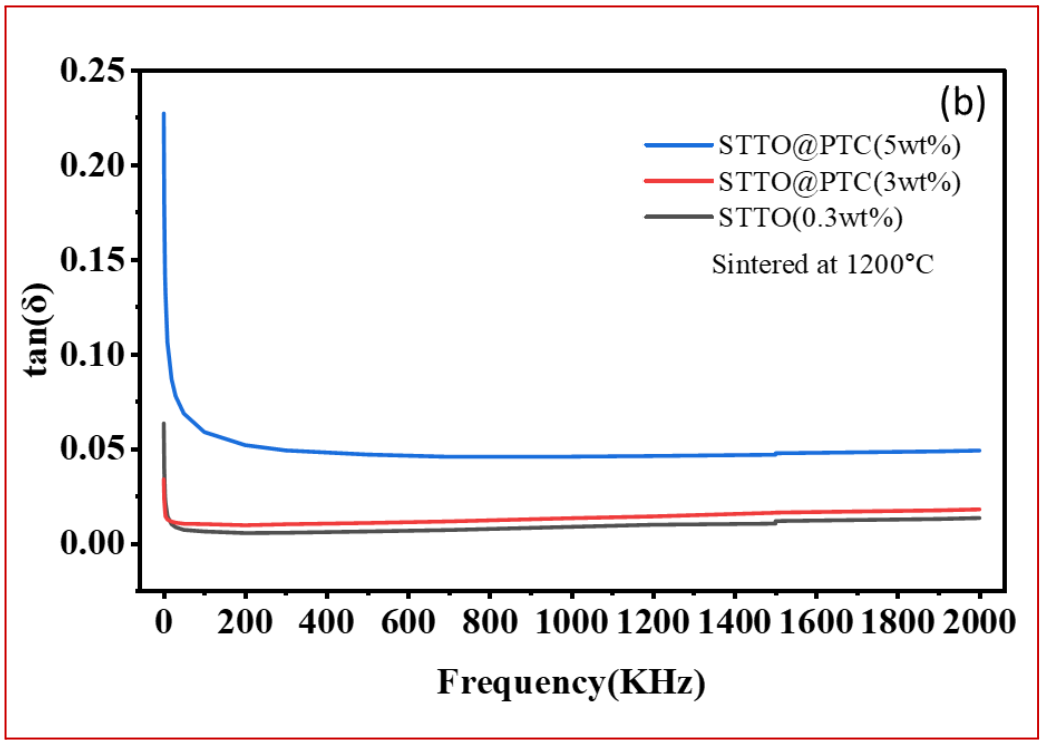

Fig. 9 (a) Deviation in the dielectric constant (K) with the frequency for STTO (0.3 wt%) , STTO@PTC (3 wt%) and STTO@PTC (5 wt%) , sintered at 1200˚C , and (b)

dielectric loss (tanδ) vs. frequency for STTO(0.3 wt%) , STTO@PTC(3 wt%) , STTO@PTC(5 wt%).

optimal microstructural balance for the STTO core. The insulating TiO_2 shell significantly reduces the macroscopic dielectric constant via the internal series capacitor effect. This specific boundary layer thickness is highly effective at physically disrupting long-range leakage currents. The performance degradation and massive loss spike observed in the 5 wt% sample further underscore that strictly limiting the shell volume fraction is critical to preventing the Maxwell-Wagner-Sillars interfacial polarization. The dielectric data indicates that the STTO@PTC (3wt%) composite successfully achieves a low-loss electrical profile for high-frequency capacitor applications [35, 40, 41].

CHAPTER 5
CONCLUSION

In summary, Ta-doped strontium titanate ($SrTi_{0.997}Ta_{0.003}O_3$; STTO) was successfully synthesized through a solid-state reaction method with pure cubic perovskite phase and verified by XRD and FTIR spectroscopy. The synthesis of a core–shell structure (STTO@PTC), validated by TEM analysis, proved to be the definite factor in optimizing dielectric performance. As the impedance spectroscopy brings out that the 0.3wt% Ta-doped $SrTiO_3$ exhibits a dielectric constant of approximately 160. The introduction of a 3wt% PTC shell results in a stable, effective dielectric constant of approximately 50. This 3wt% core–shell configuration gets a remarkable decrease in dielectric loss, maintaining a highly stable dissipation factor of $tan\delta$< 0.02 over the investigated frequency range (100Hz to 2 MHz) . This result shows superior frequency stability compared to the STTO, as the PTC shell helpfully suppresses leakage currents as well as interfacial polarization. On the other hand , experimental data suggested that exceeding this optimal shell concentration (e.g., 5wt% PTC) leads to the performance degradation, characterized by an expressive loss spike (TiO_2> 0.20) at low frequencies. These conclusions emphasize that the core–shell of STTO@PTC structure can be used for high-frequency capacitor applications, offering a highly encouraging material for next-generation , low- $tan\delta$ electronic components and high-stability energy storage systems.

For future work we will study core-shell structure dielectric properties with varying thickness of PTC coating.